

force (29) is found to correspond to their result

$$\frac{1}{16\pi c} \left[\frac{\partial}{\partial t} \{ [(\vec{\epsilon} - \vec{1})\vec{E}_1] \times \vec{B}_1^* \} + \omega \left(\frac{\partial \vec{\epsilon}}{\partial \omega} \frac{\partial \vec{E}_1}{\partial t} \right) \times \vec{B}_1^* + c.c. \right]. \quad (30)$$

Finally we give an interesting example which produces a ponderomotive magnetic field. Consider a rotating magnetic field with frequency ω , $(B_x, B_y) = B(z)(\sin\omega t, \cos\omega t)$, perpendicularly applied to the static magnetic field which is oriented in the z direction. The rotating electric field

associated with it is $(E_x, E_y) = (\omega/2c) \int B(z) dz \times (\sin\omega t, \cos\omega t)$, $E_z = [-\omega B(z)/2c](x\sin\omega t + y\cos\omega t)$. In the cold-plasma limit, the important excursion component ξ_z is given by $\frac{1}{2}(e/mc)[B(z)/\omega](x\sin\omega t + y\cos\omega t)$. We can obtain the ponderomotive magnetic field B_z^{av} directly from formulas (1), (2), and (27),

$$B_z^{av} = \frac{\partial}{\partial x} \left(A_y^{av} - c \frac{\partial \varphi^{av}}{\partial v_y} \right) - \frac{\partial}{\partial y} \left(A_x^{av} - c \frac{\partial \varphi^{av}}{\partial v_x} \right) = -\frac{1}{4} \frac{e}{mc} \frac{1}{\omega} B^2(z), \quad (31)$$

where use has been made of the fact that the contribution from $c \partial \varphi^{av} / \partial \vec{v}$ is of higher order.

In summary, we have presented a unified theory which yields a compact but general covariant form for the ponderomotive scalar and vector potentials. Its apparent compactness is a direct consequence of the introduction of the particle excursion in four-dimensional space ζ . Its generality and usefulness have been demonstrated by the direct manner in which known results are recovered and a new ponderomotive magnetic field is derived for the case of rotating rf fields.

The authors are grateful to Professor T. Taniuti and Dr. J. N. Leboeuf for their critical reading of the manuscript and valuable discussions, and to Professor A. N. Kaufman and Professor Y. C. Lee for fruitful discussions.

¹G. Hori, *Publ. Astron. Soc. Jpn.* **18**, 287 (1966).

²I. Kawakami, *J. Phys. Soc. Jpn.* **28**, 505 (1970).

³R. L. Dewar, *J. Phys. A* **9**, 2043 (1976).

⁴J. R. Cary and A. N. Kaufman, *Phys. Rev. Lett.* **39**, 402 (1977).

⁵J. R. Cary, Ph.D. dissertation, University of California at Berkeley, 1978 (unpublished), Lawrence Berkeley Laboratory Report No. 8185.

⁶S. Johnston, A. N. Kaufman, and G. L. Johnston, *J. Plasma Phys.* **20**, 365 (1978).

⁷A. N. Kaufman suggested Eq. (16), which enabled us to derive a covariant form [Eqs. (23) and (24)], although our previous analysis based upon H had led to an equivalent but not perfectly covariant form [Eqs. (1) and (2)].

⁸H. Washimi and V. I. Karpman, *Zh. Eksp. Teor. Fiz.* **71**, 1010 (1976) [*Sov. Phys. JETP* **44**, 528 (1976)].

Electron Energy Transport in Steep Temperature Gradients in Laser-Produced Plasmas

A. R. Bell, R. G. Evans, and D. J. Nicholas

Science Research Council Rutherford and Appleton Laboratories, Chilton, Didcot, Oxfordshire OX11 0QX, United Kingdom

(Received 15 September 1980)

The Fokker-Planck equation has been solved numerically in one spatial and two velocity dimensions in order to study thermal conduction in large temperature gradients occurring in laser-produced plasmas. The heat flow is an order of magnitude smaller than that predicted by the classical theory when the temperature scale length is a few electron mean free paths.

PACS numbers: 52.50.Jm, 52.25.Fi

Thermal conduction plays an important role in the transport of energy in laser-heated solid targets. The classical theory of thermal conductivity given by Spitzer and Harm¹ is derived in the limit of small temperature gradients and therefore may not be applicable to the conditions which

occur in plasmas produced by high-power lasers. It is commonly assumed that there is an upper limit to the diffusive heat flow given by $Q_{\max} = \alpha nk T(kT/m)^{1/2}$. α is a number of order unity which is not well defined but is generally taken to be about 0.6. However, this maximum heat flow

appears to be much larger than that found in experiments,² and numerical simulations give a better fit to experimental results if α is reduced to about 0.03.³ The Spitzer-Harm theory is not valid for steep temperature gradients, and it is possible that a correct treatment of electron energy transport would reveal a much lower conductivity than has previously been supposed. In this Letter, we present results of numerical simulations which examine the heat flow in temperature gradients having scale lengths a few times the electron mean free path. We find evidence for a reduction from the Spitzer-Harm conductivity by an order of magnitude.

Electron energy transport in one dimension can be described by the Fokker-Planck equation for an electron fluid in one space and two velocity dimensions:

$$\frac{\partial f}{\partial t} + v_x \frac{\partial f}{\partial x} + E \frac{\partial f}{\partial v_x} = \left(\frac{\partial f}{\partial t} \right)_{\text{collision}},$$

$$\frac{\partial E}{\partial x} = r \left[\int f d^3 v - 1 \right].$$

f , the electron distribution function in phase space, is a function of the spatial dimension x , the magnitude of the velocity v , and the angle θ the velocity makes with the x direction. r is a factor less than unity introduced into the numerical model in order to make the plasma oscillation period comparable with the time step needed to model collisions. The ions are assumed to be immobile. The equation is made dimensionless by expressing time in units of ω_p^{-1} and length in units of the Debye length λ_D of a plasma at a temperature $kT/m = 1$, i.e., $\langle v^2 \rangle = 3$. The collision term is given by the Rosenbluth-MacDonald-Judd theory as described by Dolinsky⁴ and by Tidman and Eviatar.⁵ The collision coefficients (T and F in Ref. 5) are calculated in the approximation that the electron velocity distribution is isotropic. This is a good approximation since most of the electrons are relatively slow and collisional. Only the few electrons on the thermal tail are strongly anisotropic and they do not contribute greatly to the collision coefficients. Electron scattering by ions is included but energy exchange between electrons and ions is slow and has been omitted.

The equations are solved numerically⁶ by expressing f as an expansion of Legendre polynomials in $\cos \theta$. Advection is modeled on the solution of the advective equation given by Cheng and Knorr,⁷ and f is interpolated in x by cubic splines. The motions in the v dimension are modeled on

the scheme given by Chang and Cooper⁸ which is implicit and conserves particles. Acceleration in the self-consistent electric field is solved explicitly.

The program was used to simulate the propagation of a heat front across a plasma with $Z = 4$. The plasma is initially uniform in density and temperature and is quickly heated to 4 times its initial temperature throughout a region $0 < x < 350$ at one end of the spatial grid. The heat source is such as to maintain the high temperature in this region thereafter, injecting sufficient heat to balance the loss of heat to the cold plasma by conduction. The program was run with 64 spatial grid points at intervals of $\Delta x = 34.71$, 32 velocity grid points at intervals $\Delta v = 0.2$, and a Legendre polynomial expansion of eight terms. The time step was $\Delta t = 5.26$. The electric field was reduced by a factor $r = 0.0011$ and the number of electrons in a Debye sphere was $N_D = 100$. These parameters give $t_s(v) = 2.0v^3 \Delta t$ and $\lambda(v) = 0.3v^4 \Delta x$, where $t_s(v)$ is the scattering time for an electron with velocity v defined here as

$$t_s(v) = 3N_D v^3 / (Z + 1) \ln(3N_D),$$

and $\lambda(v) = vt_s(v)$ is the electron mean free path.

Figure 1 follows the evolution of the temperature and heat-flow distributions. The temperature is given as the mean-square velocity and the heat flow Q is equal to $0.5nm\langle v^2 v_x \rangle$. The temperature gradient is initially spread over the order of a mean free path and extends further into the plasma as time progresses. The maximum heat flow always occurs at the boundary of the heated region where typically $\langle v^2 v_x \rangle \sim 0.2$ and $\langle v^2 \rangle \sim 3.5$.

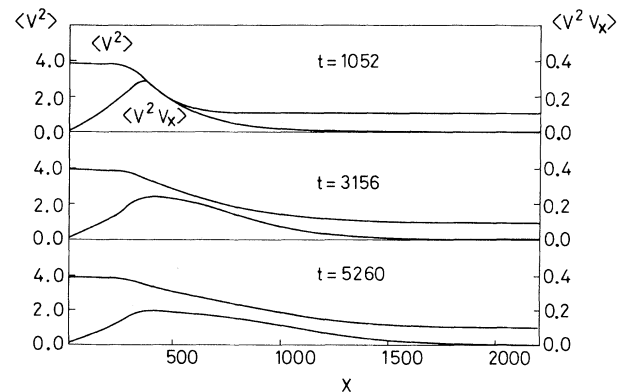


FIG. 1. Plots of $\langle v^2 \rangle$ (temperature) and $\langle v^2 v_x \rangle$ (heat flow) as functions of x at times $t = 1052$, 3156, and 5260. The plasma is heated in the region $x < 350$.

These values imply a heat flow $Q \sim 0.1nkT(kT/m)^{1/2}$.

For a more exact analysis of the results, the heat flow along the temperature gradient can be compared with that given by the Spitzer-Harm theory by plotting the heat flow Q divided by the local free-streaming limit $Q_f = nkT(kT/m)^{1/2}$ against L/λ the local inverse temperature gradient [$L = T/(dT/dx)$] in mean free paths. The Spitzer-Harm conductivity of a plasma with $Z = 4$ is $Q = 3.64Q_f \lambda/L$. Figure 2 plots Q/Q_f against L/λ at successive grid points along the heat front at times $t = 2630$ and $t = 5260$. The points can be read from the bottom right where they relate to the hot end of the grid, following the line of points to the top left, corresponding to the top of the heat front, and then back to the right along the upper curves where they correspond to data at the bottom of the heat front at large x . The left-most point always corresponds to the first grid point immediately to the right of the heated region. Defined in this way, the thermal conductivity at the base of the heat front exceeds the Spitzer-Harm conductivity. The large heat flow there is carried by hot, nearly collisionless, electrons streaming away from the top of the heat front while the free-streaming limit is determined by the initial population of unheated electrons. On the other hand, the values of Q/Q_f in the heated region (the lower line of points) are much lower than at the base of the front for similar values of L/λ . However, it is the heat flow on the main body of the heat front which determines its overall progress into

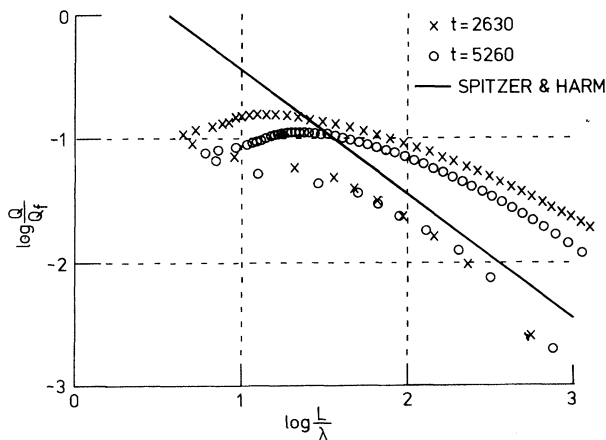


FIG. 2. Plot of heat flow Q against inverse temperature gradient. $Q_f = nkT(kT/m)^{1/2}$, λ is the mean free path of an electron with energy $\frac{3}{2}kT$, and $L = T(dT/dx)^{-1}$. All quantities are defined locally. The solid line gives the Spitzer-Harm conductivity for $Z = 4$.

the plasma, and this is given by the first few points on the left of Fig. 2. The heat flow there is an order of magnitude less than the free-streaming limit. There is a tendency for the conductivity to decrease as the elapsed time becomes large compared with the angular-scattering time $t_s(v = 3) \approx 300$ and then the energy-loss time $t_L(v = 3) \approx 1400$. The relatively steady state which occurs at large times is more relevant to laser plasmas in which the heat flow is partially balanced by convection of the plasma fluid.

These results show that, in the presence of steep temperature gradients, the heat flow at any one point is not simply a function of the local plasma state but is determined by the velocity distribution over a region which is a few mean free paths thick. The large scatter of points for any given L/λ when measured at different times or points on the heat front indicates that we cannot obtain a unique expression for the thermal conductivity. Nevertheless, it is clear that the heat flow is an order of magnitude less than that given by the Spitzer-Harm theory where it is important, on the main body of the heat front. Hence, we have evidence of "flux inhibition" when the scale length of the temperature gradient is a few times the electron mean free path.

The reason for the low thermal conductivity becomes clear if we consider the velocity distribution calculated by Spitzer and Harm which takes the form $f(v, x, \theta) = f_0(v, x) + f_1(v, x)\cos\theta$. The heat

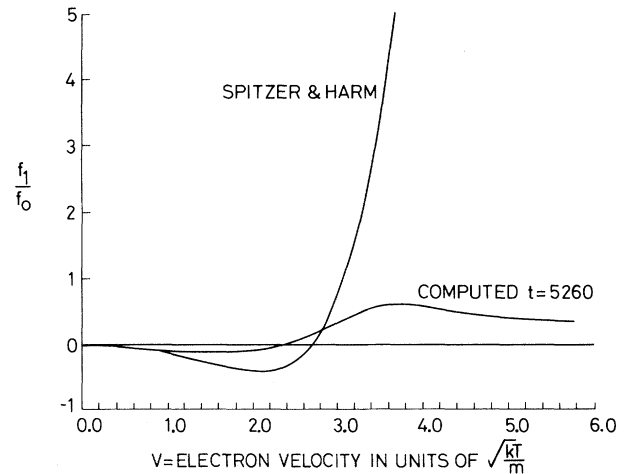


FIG. 3. Comparison of the computed f_1/f_0 with the curve given by Spitzer and Harm for the same temperature gradient. The distribution is plotted at time $t = 5260$ and at the position immediately to the right of the heated region where the heat flow is at its maximum.

flow is mainly carried by a small number of electrons on the tail of the Maxwellian distribution. As pointed out by Gray and Kilkenny,⁹ f_1/f_0 exceeds unity at velocities for which the energy flux is large when λ/L is of the order 0.01, and the linearized theory breaks down since f is then negative. Figure 3 plots the ratio f_1/f_0 as given by the simulation when $t=5260$ at the point immediately to the right of the heated region where the heat flow is largest. f_1/f_0 as given by the Spitzer-Harm theory is plotted for comparison and two major differences are apparent: (a) The simulation curve does not rise to values much larger than unity and (b) since f_1 is much lower at high velocities in the simulation, f_1 need not take such large negative values at low velocities to provide the return current. The limitation of f_1/f_0 to around unity reduces the large heat flow which peaks at velocities around $4(kT/m)^{1/2}$ in the Spitzer-Harm theory thus reducing the overall heat flow by an order of magnitude.

We are grateful to Dr. A. B. Langdon, Lawrence

Livermore Laboratory, and Dr. R. J. Mason, Los Alamos Scientific Laboratory, for stimulating discussions.

¹L. Spitzer and R. Harm, Phys. Rev. **89**, 977 (1953).

²W. L. Kruer, Comments Plasma Phys. Controlled Fusion **5**, 69 (1979).

³R. C. Malone, R. L. McCrory, and R. L. Morse, Phys. Rev. Lett. **34**, 721 (1975).

⁴A. Dolinsky, Phys. Fluids **8**, 436 (1965).

⁵D. A. Tidman and A. Eviatar, Phys. Fluids **8**, 2059 (1965).

⁶A. R. Bell, R. G. Evans, and D. J. Nicholas, Rutherford and Appleton Laboratories Report No. RL/80/049, 1980 (unpublished).

⁷C. Z. Cheng and G. Knorr, J. Comp. Physiol. **22**, 330 (1976).

⁸J. S. Chang and G. Cooper, J. Comp. Physiol. **6**, 1 (1970).

⁹D. R. Gray and J. D. Kilkenny, Plasma Phys. **22**, 81 (1980).

Nonlinear Magnetic Islands and Anomalous Electron Thermal Conductivity

V. P. Pavlenko^(a) and J. Weiland

Institute for Electromagnetic Field Theory, Chalmers University of Technology, S-412 96 Göteborg, Sweden

(Received 17 November 1980)

It is found that nonlinear magnetic islands are formed, in an inhomogeneous magnetized plasma, in the presence of a longitudinal current. These magnetic islands may cause an enhanced electron thermal conductivity in a turbulent plasma state.

PACS numbers: 52.25.Fi, 51.60.+a

One of the most central points in the understanding of transport processes in fusion devices is the anomalous electron thermal conductivity. Recently, it was suggested that the mechanism of this conductivity is the thermal motion of electrons along the magnetic field lines which are perturbed by a two-dimensional, extremely low-frequency electromagnetic mode.¹ Because this mode has a negligible electric field, it was called the magnetostatic mode.

The transport due to the magnetostatic mode in a homogeneous plasma was studied by several authors.¹⁻⁴ It was found that the anomalous electron diffusion is comparable to the classical in thermal equilibrium. In a turbulent plasma, however, the diffusion may exceed the classical by several orders of magnitude. In a nonuniform

plasma it turns out that the magnetostatic mode obtains a real frequency which is of the order of the electron diamagnetic drift frequency ω_* .⁵ As we will show, this real frequency strongly influences the diffusion. Following the procedure of Chu, Chu, and Ohkawa,¹ we can write the diffusion coefficient in the form

$$D = \frac{v_{th}^2}{(2\pi)^2 B_0^2} \int \langle B_k^2 \rangle \frac{\gamma_k}{\omega_k^2 + \gamma_k^2} d^3k, \quad (1)$$

where v_{th} is the electron thermal velocity, B_0 is a uniform background magnetic field, B_k is the Fourier component of the transverse-magnetic-field perturbation, ω_k is the real part of the eigenfrequency and $1/\gamma_k$ is the decorrelation time. Clearly ω_k will strongly decrease the diffusion if it is larger than γ_k . For comparison we may con-